Supplementary Information for

Charge doping induced reversible multistep structural phase transitions and electromechanical actuation in two-dimensional 1T'-MoS_2

Kaiyun Chen,[a] *Junkai Deng,**[a] *Qian Shi,*[a] *Xiangdong Ding,*[a] *Jun Sun,*[a] *Sen Yang,**[a] *and Jefferson Zhe Liu**[b]

[a]MOE Key Laboratory for Nonequilibrium Synthesis and Modulation of Condensed Matter, State Key Laboratory for Mechanical Behavior of Materials, Xi'an Jiaotong University, Xi'an 710049, China
E-mail: junkai.deng@mail.xjtu.edu.cn; yangsen@mail.xjtu.edu.cn

[b]Department of Mechanical Engineering, The University of Melbourne, Parkville, VIC 3010, Australia
E-mail: zhe.liu@unimelb.edu.au

This PDF file includes:

Supplementary Note 1: Total energy correction of charged MoS_2 slab models in DFT calculations

In DFT calculations of a charged slab using Vienna Ab-initio Simulation Package (VASP), a homogeneous opposite charge will be automatically added in the background of supercells to keep the system electric neutral. However, both the slab charges and the background charges contribute to the calculated total energy values (under the periodic boundary condition). Thus, the reliability of using direct total energy results from VASP to assess the phase stability remains an open question. To address this problem, in 2016, Reed group proposed a correction method.[1] Using this method, they predicted a phase transition from 2H to 1T' in $MoTe_2$ under electrostatic gating based on VASP calculations. In 2017, Wang et al confirmed this predicted phase transition in the experiment.[2] This validated the correction method from the Reed group. In this manuscript, we also adopted this method to verify the phase transition from 1T' to 1T (results shown in Fig. 2a). The details are presented below.

For a charged slab, the uniform background charge will induce additional background potential V_{bg}. It should be subtracted from the total potential V_{total}. The background potential V_{bg} is given according to Gauss theorem:

$$V_{bg}(Q',z) = \frac{Q'}{2\varepsilon_0 AL}(Z^2 - \frac{1}{4}L^2) \quad (1)$$

where Q' is the uniform compensating background charge, A is the area of the slab, ε_0 is the permittivity of vacuum and L is the distance between slabs (due to the periodic boundary condition) along z-direction (perpendicular axis). In addition to the background charge induced potential, the uniform electric field on two adjacent slab images should be restored, which is $Q'/(2\varepsilon_0 A)$ according to Gauss theorem. The rest should be the intrinsic potential from the charged slab.

In Reed's method, the total energy of a charged slab (or 2D material) can be expressed as:

$$E_{total}(Q, z_{ref}) = E_0 + \int_0^Q \Delta V(Q', z_{ref}) dQ' \quad (2)$$

where E_0 is the ground state energy of electrically neutral monolayer, the integral is the energy of moving charge Q form the reference position to Fermi level, and $\Delta V(Q', z_{ref})$ is the potential difference between the reference position z_{ref} and the surface of the material as z_f. In this calculation, z_f is taken to be the plane at which Kohn-Sham potential is equal to the Fermi level, as shown in Fig. S1(a).

The potential difference in Eq. (1) is:

$$\Delta V(Q', z_{ref}) = [V_{tot}(Q', z_{ref}) - \mu_f(Q')] - [V_{bg}(Q', z_{ref}) - V_{bg}(Q', z_f(Q'))] + \frac{Q'}{2\varepsilon_0 A}[z_{ref} - z_f(Q')] \quad (3)$$

All the quantities in Eq. (3) can be determined in DFT calculations. Fig. S1(b) summarizes the variation of the calculated ΔV as a function of charge Q'. The discontinuity (~0.1 V) at Q = 0.10 h^+/atom in Fig. S1 is due to the phase transition from 1T' to 1T. We can use a linear fitting these two parts respectively to approximate the relation:

$$\Delta V(Q', z_{ref}) = a + bQ' \quad (4)$$

Substituting Eq. (4) into Eq. (2) yields the corrected total energy of the charged slabs. According to Reed's works, these corrected total energy results can be used to investigate the phase transition.

Supplementary Note 2: The possibility of strain induced phase transition among 1T, $1T_t$' and 1T'

The injection of charge can change both the total energy and the equilibrium lattice constants of MoS_2. It is interesting to examine whether the strain itself could induce phase transition and the new phase $1T_t$'. We did DFT calculations of 1T' phase under a tensile or compressive strain without hole doping. Fig. S6 shows the new results. Note that the $D_{Mo1\text{-}Mo2}/D_{Mo2\text{-}Mo3}$ value is always smaller than that of 1T ($D_{Mo1\text{-}Mo2}/D_{Mo2\text{-}Mo3} = 1$) and $1T_t$' ($D_{Mo1\text{-}Mo2}/D_{Mo2\text{-}Mo3} \approx 0.85$). The total energy curve is smooth without any abrupt changes as those seen in Fig. 3. Thus, we can conclude that MoS_2 remains in 1T' phase and does not exhibit phase transition under strains without charge doping.

References:

1 Y. Li, K. A. Duerloo, K. Wauson and E. J. Reed, *Nat. Commun.*,2016, **7**, 10671.
2 Wang, Y., Xiao, J., Zhu, H. et al. *Nature*, 2017, 550, 487–491.
3 M. Kan, J. Y.Wang, X.W. Li, S. H. Zhang, Y.W. Li, Y. Kawazoe, Q. Sun and P. Jena, *J. Phys. Chem. C*, 2014, 118, 1515–1522.

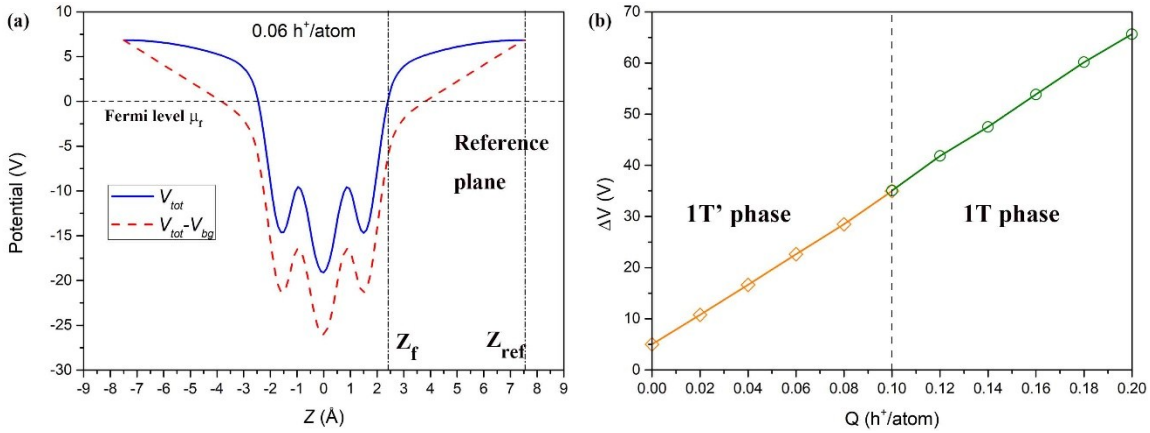

Fig. S1 (a) Electronic Kohn-Sham potential profile of a charged monolayer MoS_2 (0.06 h^+/atom) calculated using PBE-DFT. (b) The potential difference with Q increasing.

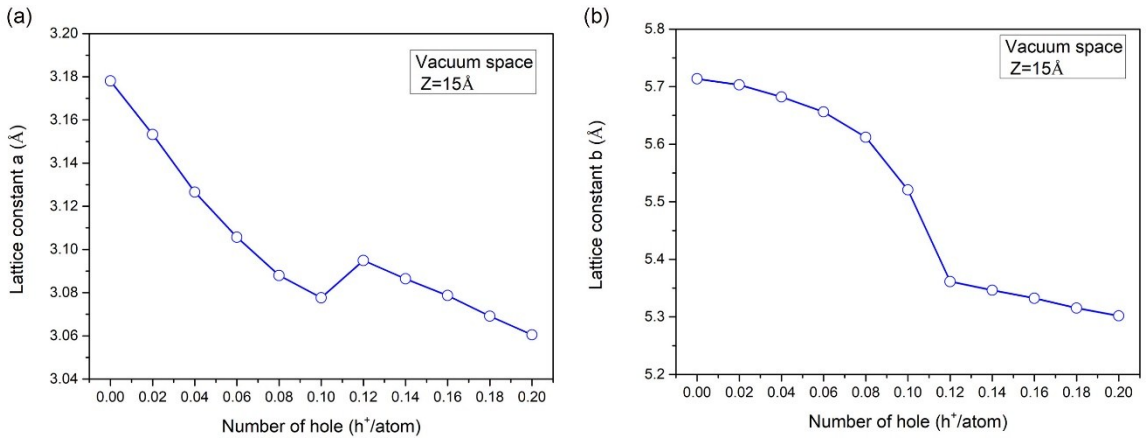

Fig. S2 Lattice constants of 1T'-MoS_2 as function of hole injection. The supercell has a size of 15 Å in *z*-direction. A sudden change can be observed close to 0.10 h^+/atom. This represents 1T' to 1T phase transition.

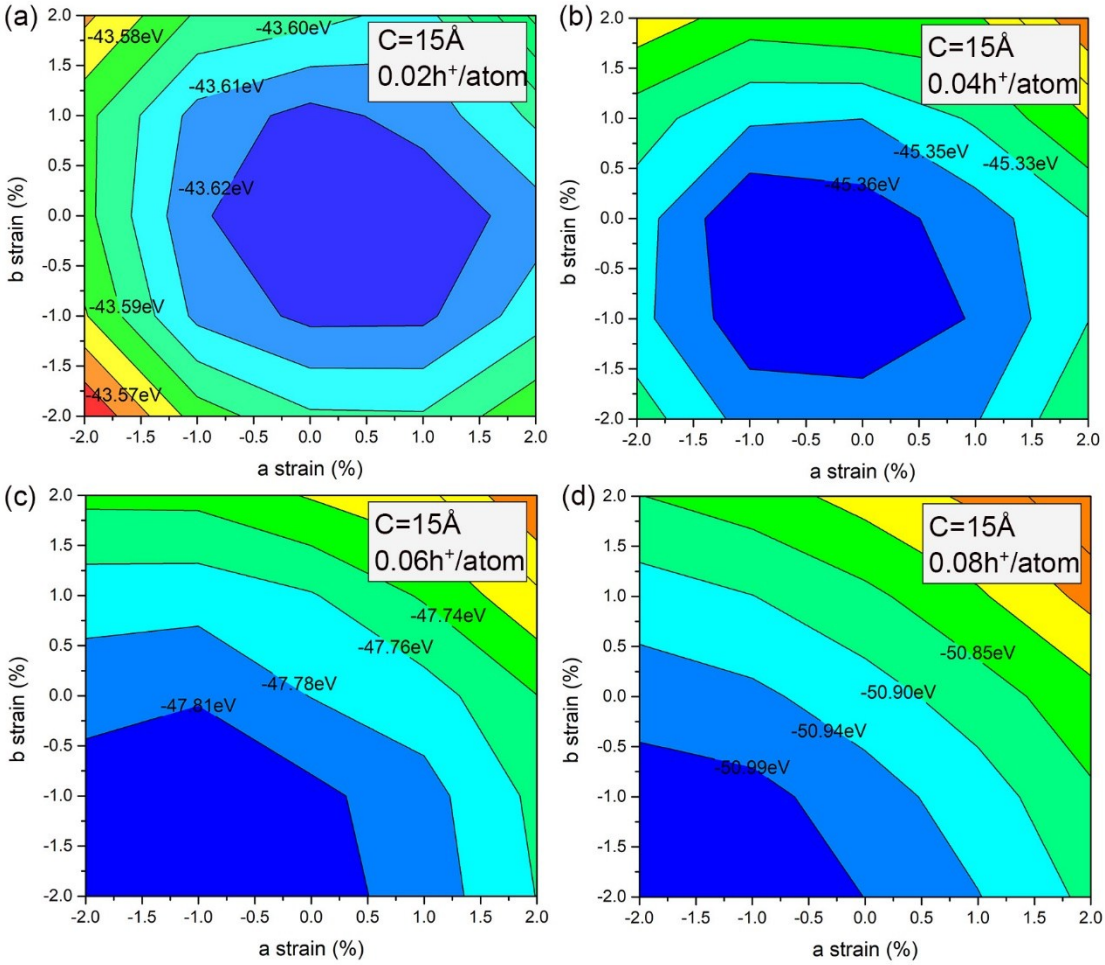

Fig. S3 The total energy of hole doped MoS_2 as a function of fixed in-plane strain ε_x and ε_y. The hole doping level is (a) 0.02, (b) 0.04, (c) 0.06 and (d) 0.08 h^+/atom, respectively. The supercell used in our calculation has a size of 15 Å in *z*-direction. The lattice constants *a* and *b* are fixed in a range from –2% to 2% compared with neutral state. All energies are corrected by using the method proposed by Reed. It can be clearly seen that both lattice constants *a* and *b* decrease as the positive charge increasing.

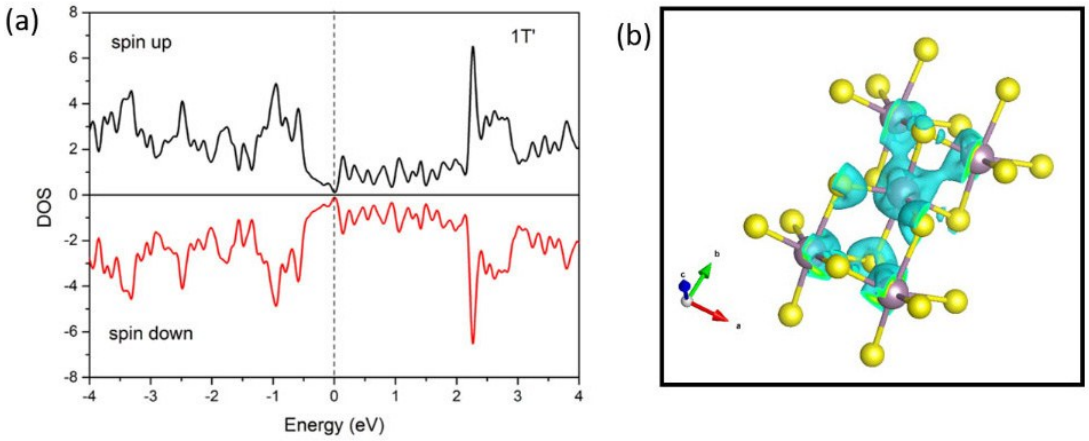

Fig. S4 Electron structure of 1T' MoS_2. (a) DOS of 1T'-MoS_2. (b) Partial electron density distribution ranges –1.5eV to Fermi level, clearly showing the Mo-Mo dimer bonds.

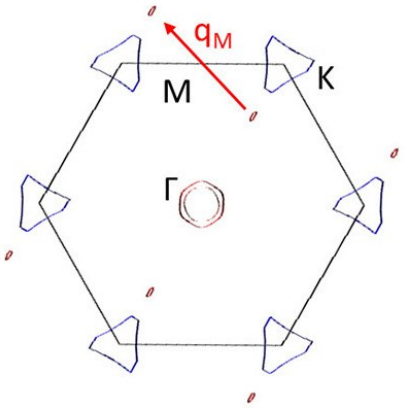

Fig. S5 Fermi surface of monolayer 1T-MoS_2. The red and blue pockets stand for electron and hole Fermi surface, respectively. The nesting vector q_M connects the electron pockets (solid red line), demonstrating the instability of 1T-MoS_2.

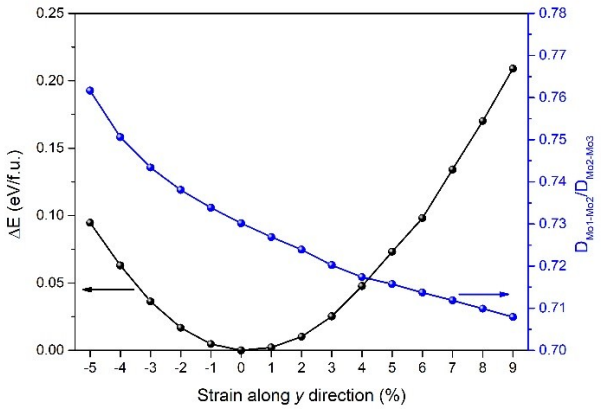

Fig. S6 The energy and $D_{Mo1\text{-}Mo2}/D_{Mo2\text{-}Mo3}$ of 1T' under tensile and compressive strain. In this process, any spontaneous phase transition from 1T' to 1T or $1T_t$' cannot be observed. while $1T_t$' and 1T phase will transit to 1T' after relaxation without charge doping.

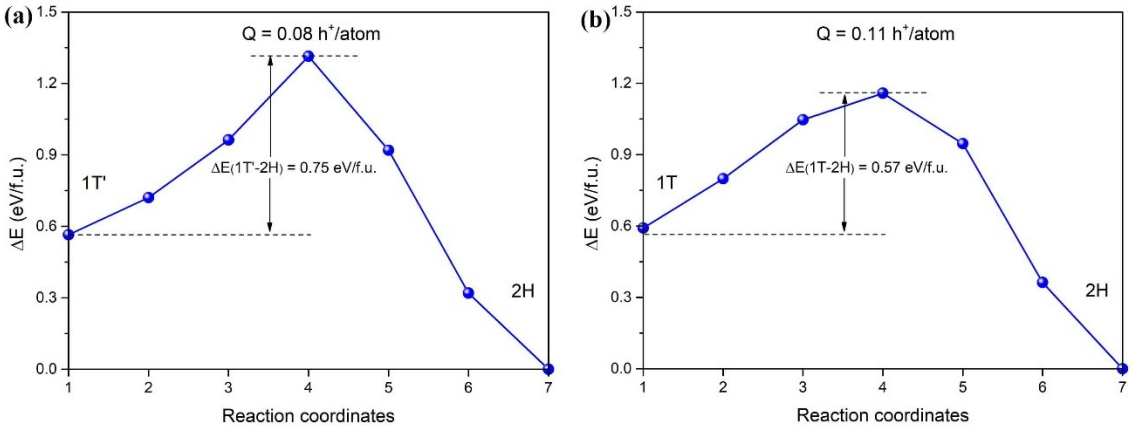

Fig. S7 Relative total energy profile along the phase transition pathway among 1T, 1T' and 2H phases. (a) Energy barrier between 1T' and 2H phase at Q = 0.08 h^+/atom. (b) Energy barrier between 1T and 2H phase at Q = 0.11 h^+/atom. The climbing image nudged elastic band (CI-NEB) method was used in these calculations.

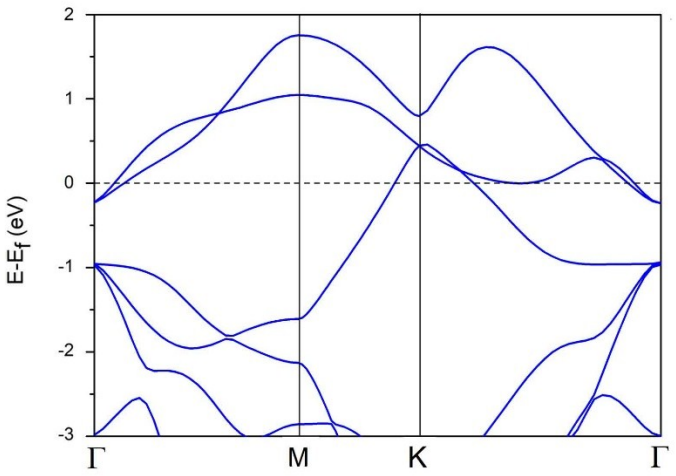

Fig. S8 Band structure of electro-neutral 1T phase using GGA-PBE functional. The paths of band structures with PBE are consistent to previous study using HSE06 functional.[3] The results are very similar. This indicates that GGA-PBE is good for our case.

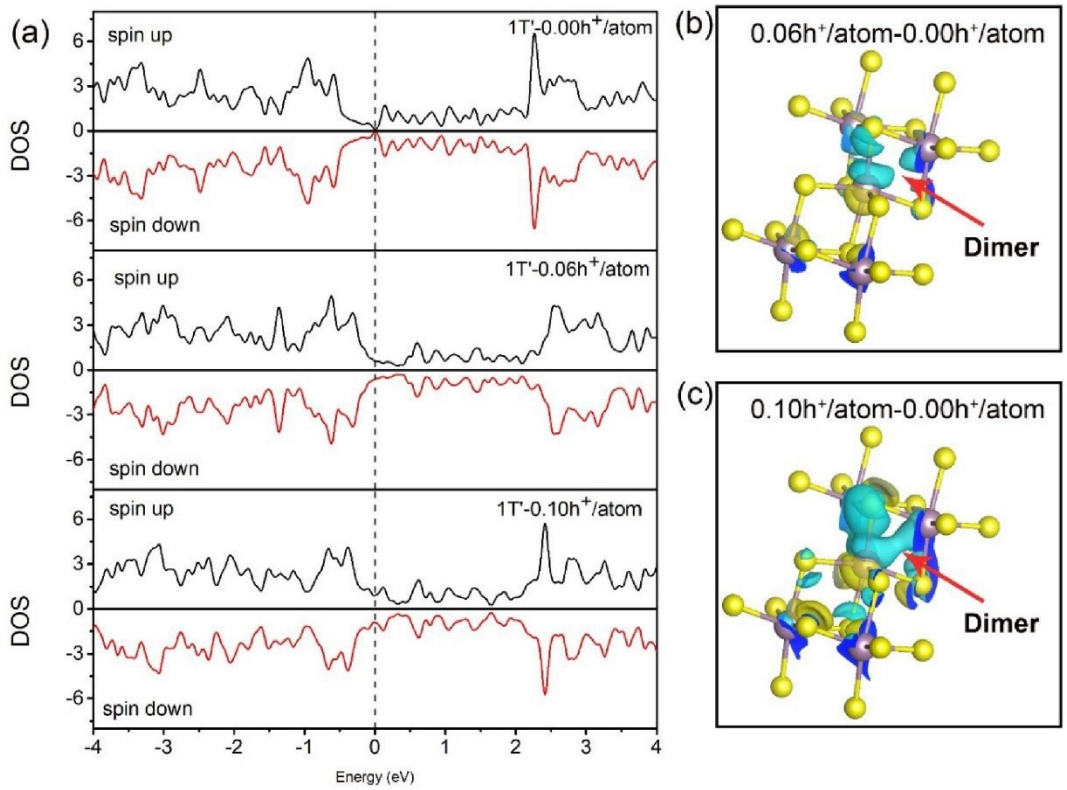

Fig. S9 Electron structures of 1T'-MoS_2 with hole injection. (a) Electronic density of states (DOS) under different hole injection. (b) and (c) show excess charge distribution for the 0.06 h+/atom and 0.10 h^+/atom cases, respectively. The blue color represents electron depletion.

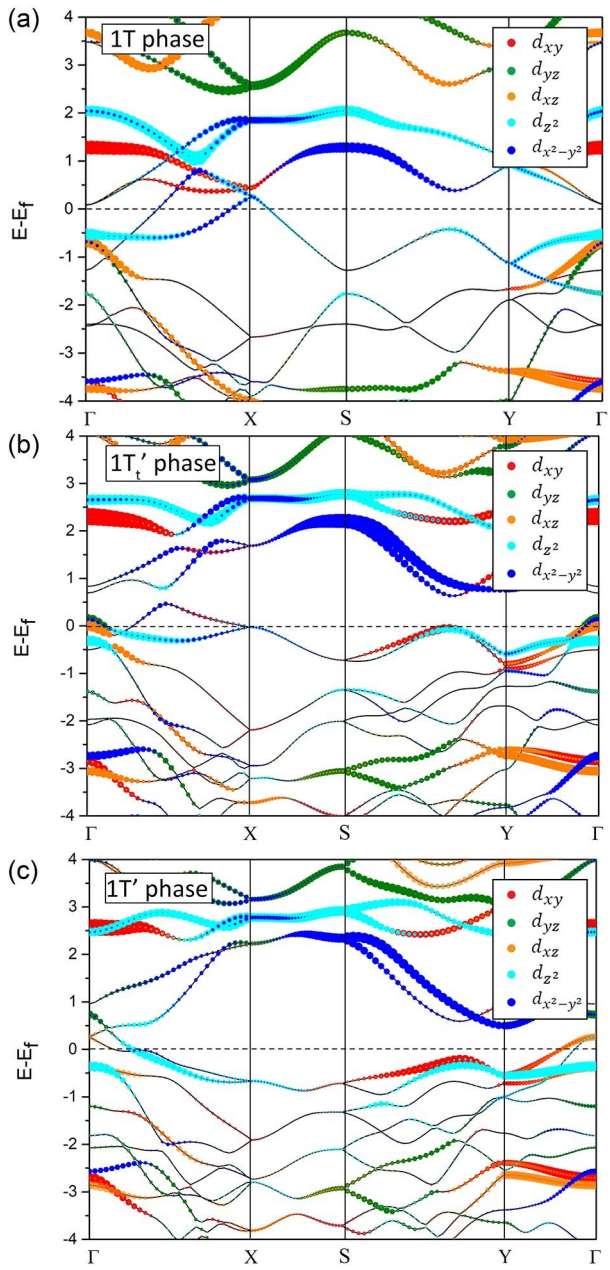

Fig. S10 Electron band structures of 1T, 1T$_t$' and 1T' under Q = 0.09 h$^+$/atom. The *d* orbitals of Mo atom are mapped with different colors: d_{xy}, red; d_{yz} , green; d_{xz}, orange; d_{z^2}, cyan; $d_{x^2-y^2}$, blue.

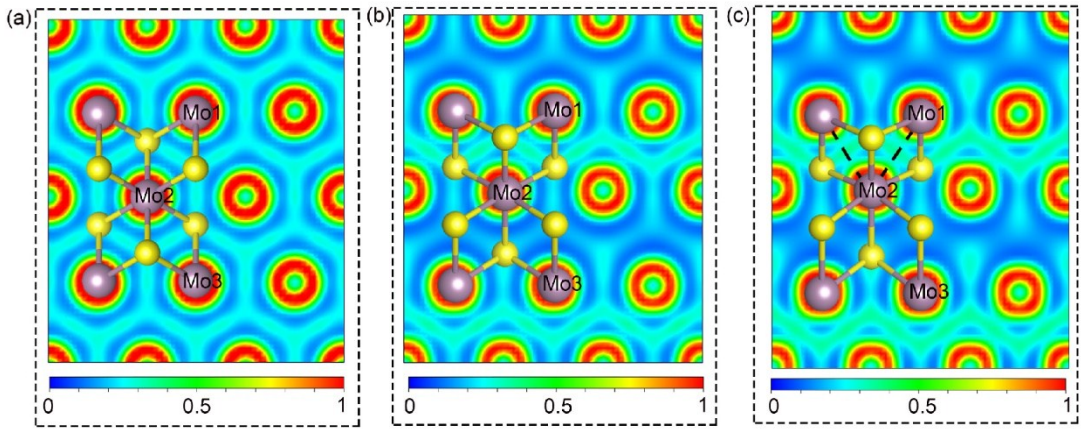

Fig. S11 Electron local function (ELF) of 1T, $1T_t$' and 1T' phase with Q=0.09h^+/atom for (a) 1T, (b) $1T_t$', and (c) 1T'. The $1T_t$' has ELF results similar to that of 1T'.

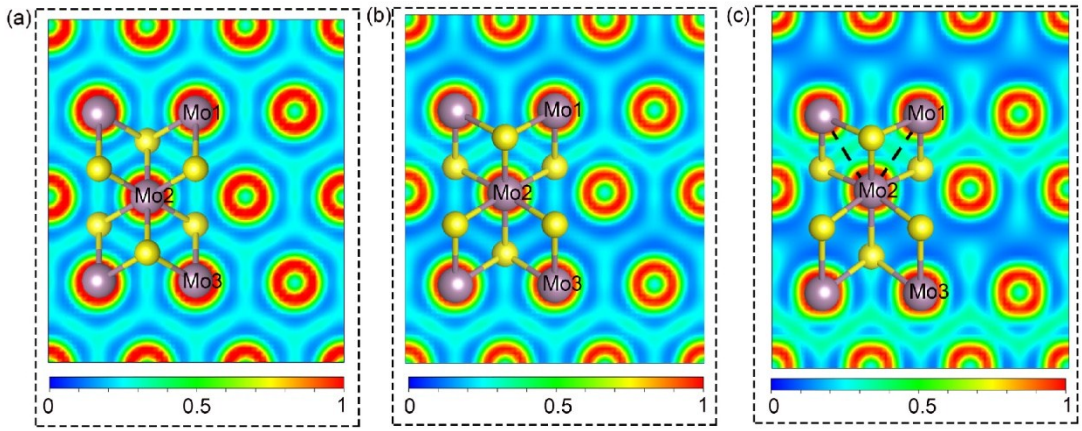

Fig. S12 Electron local function (ELF) of 1T, $1T_t$' and 1T' phase with Q=0.10 h^+/atom. The $1T_t$' has ELF results similar to that of 1T instead of 1T'.

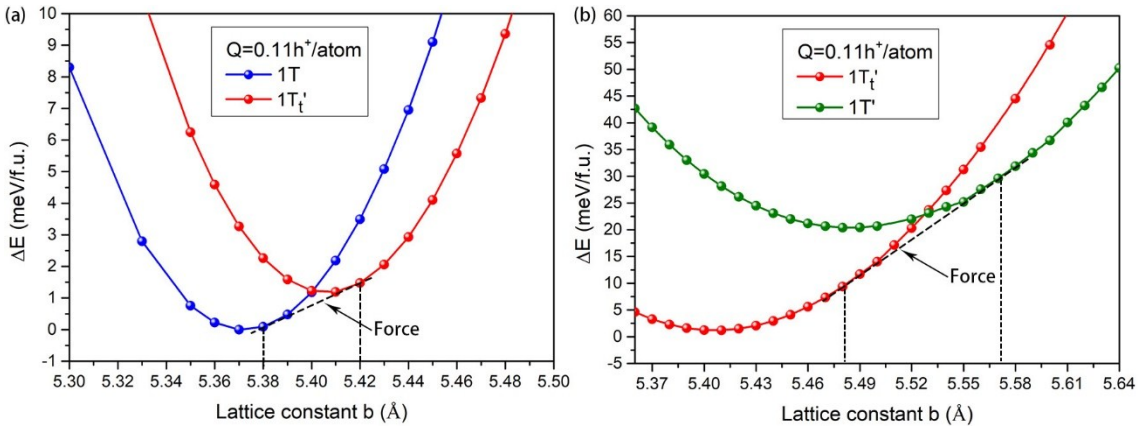

Fig. S13 Relative total energy of MoS_2 versus lattice constant along *y* direction under Q=0.11 h^+/atom. (a) The energy change with the change of lattice constant *b*. (b) The energy change with the change of lattice constant *b*. Note that Helmholtz free energy equals to total energy at zero Kelvin. The common tangent line is used to determine the critical stress for phase transition. This method is used to construct the stress–strain relation in Fig. 5b, *i.e.*, superelasticity under stress–control condition.

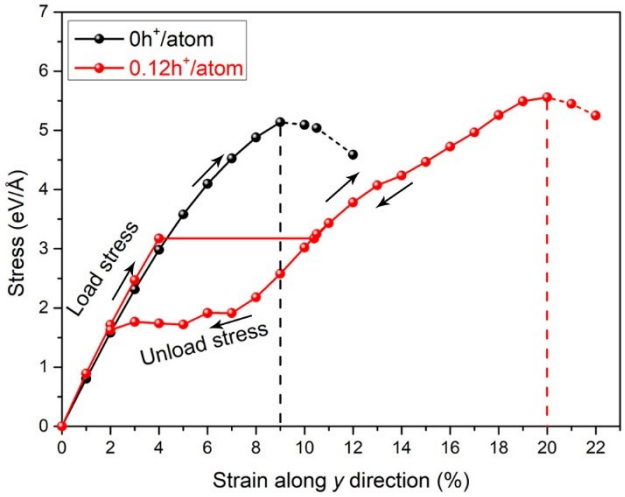

Fig. S14 Stress-strain relation of MoS_2 (uniaxial tension in *y*-direction) under zero or 0.12 h^+/atom hole injection. The plateau corresponds to the 1T to 1T' phase transition. Only one plateau is observed in contrast to Fig. 5.